CHEMISTRY OF MATERIALS
Article

Chem. Mater. **2010,** *22,* 1059–1070 1059
DOI:10.1021/cm902023h

Crystal Structure and Electrochemical Properties of A_2MPO_4F Fluorophosphates (A = Na, Li; M = Fe, Mn, Co, Ni)†

Brian L. Ellis,‡ W. R. Michael Makahnouk,‡ W. N. Rowan-Weetaluktuk,§ D. H. Ryan,§ and Linda F. Nazar*,‡

‡*University of Waterloo, Department of Chemistry, 200 University Avenue West, Waterloo, Ontario, Canada N2L 3G1, and* §*Department of Physics, McGill University, 3600 University Street, Montreal Quebec Canada H3A 2T8*

Received July 6, 2009. Revised Manuscript Received September 9, 2009

We report new solid state and hydrothermal synthetic routes to $(Li,Na)_2FePO_4F$ that incorporate carbon-containing additives and result in good electrochemical properties of this Li (or Na) ion electrode material. Single crystal X-ray diffraction analysis of Na_2FePO_4F prepared by flux growth confirms the unusual structural features of this compound that include pairs of face-sharing metal octahedra and [6 + 1] coordination of the sodium ions. Facile Na−Li ion-exchange occurs upon reflux with lithium salts, upon electrochemical cycling in a cell (vs. Li), and also in a cell simply equilibrated at OCV. The material does not exhibit typical two-phase behavior on electrochemical cycling. A combination of a redox process which occurs with little structural strain, and ion scrambling give rise to a solid solution-like sloping voltage profile on charge−discharge, although localization of the $Fe^{2+/3+}$ in the mixed valence single phase intermediate, $Na_{1.5}FePO_4F$ drives a very small structural distortion. Temperature-dependent Mössbauer spectroscopy measurements confirm this localization, at least on short time scales (10^{-8} s), which persists to 370 °C. Finally, polycrystalline powders of other members of this family of compounds (Na_2CoPO_4F, Na_2NiPO_4F) were synthesized for the first time. Na_2CoPO_4F has a Co^{2+}/Co^{3+} potential near 4.8 V. Mixed-metal phosphates of the form $Na_2(Fe_{1-x}M_x)PO_4F$, where M = Co, Mg, were also synthesized and found to be promising positive electrode materials for Li-ion or Na-ion energy storage devices.

Introduction

Iron phosphates have been vigorously pursued as environmentally friendly and inexpensive positive electrode materials for lithium-ion batteries since their initial report in 1997.[1] Their low cost and environmentally benign nature, coupled with cell potentials ranging from 2.8 to 3.4 V, stable cycling capacity, and good safety characteristics make them highly desirable for energy storage devices. The only member of the family to reach prominence is $LiFePO_4$, which crystallizes in an olivine structure and exhibits a theoretical gravimetric capacity of 170 mAh/g. Electron transport is closely correlated to ion transport in this material,[2] predominately along 1-D tunnels although other pathways have been suggested.[3,4] As a consequence of the high electron-ion correlation and large volume change, a two-phase boundary is formed upon oxidation, which can limit the kinetic performance of the material. A solid solution regime exists at room temperature near the end-members ($Li_\alpha FePO_4$ and $Li_{1-\beta}FePO4$),[5] the extent of which increases with decreasing dimensions of the crystallites. Although highly defective nanoparticles also apparently exhibit solid solution behavior,[6] such behavior is only observed in bulk particles if compounds of the type $Li_{1-x}FePO_4$ are heated to high temperature (> 200 °C).[2,7] In contrast, the two-dimensional material, $(Na,Li)_2FePO_4F$ exhibits quasi-solid solution behavior at room temperature, as we have previously reported.[8]

Although fundamental questions of solid solution behavior, lattice elasticity and ionic transport in two-dimensional systems are raised in consideration of $(Na,Li)_2FePO_4F$, it is also of interest in a more practical context. Of late, concerns have surfaced of the resource availability of lithium and hence future cost, in light of the projected orders-of-magnitude increase in lithium usage in batteries for low emission hybrid and electric vehicles. Most untapped lithium reserves occur in remote or

† Accepted as part of the 2010 "Materials Chemistry of Energy Conversion Special Issue".

*To whom correspondence should be addressed. E-mail: lfnazar@uwaterloo.ca.

(1) Pahdi, A. K.; Nanjundaswamy, K. S.; Goodenough, J. B. *J. Electrochem. Soc.* **1997**, *144*, 1188–1194.
(2) Ellis, B.; Perry, L. K.; Ryan, D. H.; Nazar, L. F. *J. Am. Chem. Soc.* **2006**, *128*, 11416–11422.
(3) Li, J.; Wenlong, Y.; Martin, S.; Vaknin, D. *Solid State Ionics* **2008**, *179*, 2016–2019.
(4) Amin, R.; Balaya, P; Maier, J. *Electrochem. Solid-State Lett.* **2007**, *10*, A13–A16.
(5) Yamada, A.; Koizumi, H.; Nishimura, S.-I.; Sonoyama, N.; Kanno, R.; Yonemura, M.; Nakamura, T.; Kobayashi, Y. *Nat. Mater.* **2006**, *5*, 357–360.
(6) Gibot, P.; Casas-Cabanas, M.; Laffont, L.; Levasseur, S.; Carlach, P.; Hamelet, S.; Tarascon, J.-M.; Masquelier, C. *Nat. Mater.* **2008**, *7*, 741–747.
(7) Delacourt, C.; Poizot, P.; Tarascon, J.-M.; Masquelier, C. *Nat. Mater.* **2005**, *4*, 254–260.
(8) Ellis, B.; Makahnouk, W. R. M.; Makimura, Y.; Toghill, K.; Nazar, L. F. *Nat. Mater.* **2007**, *6*, 749–753.

Published on Web 11/13/2009

politically sensitive areas.[9] While the debate over the feasibility and environmental impact of lithium carbonate production continues, sodium-based compounds are under consideration as options for large scale energy storage coupled to renewable energy sources, for example. Regarding the anode for such batteries, it has been demonstrated that sodium may be intercalated into hard carbon. Capacities of 350 mAh/g have been achieved.[10] As such, sodium-based redox compounds may be used as intercalation electrodes in various systems. It was also shown recently that the tavorite $NaVPO_4F$ (isostructural with $LiVPO_4F$[11]) can be used as the positive electrode in a cell coupled to a negative electrode based on either metallic lithium or sodium or on a hard carbon.[12,13]

In our first report on Na_2FePO_4F, we showed that this new material functions smoothly as a positive electrode material in a coin cell using lithium salt electrolytes (with an appropriate negative electrode), and proposed that it would also serve well in a sodium ion cell. In a lithium-ion cell, one mobile Na is rapidly exchanged for Li. The compound has a theoretical capacity of 135 mAh/g in the form (Na,Li)$FePO_4F$ and the electrochemical profile displays quasi solid-solution behavior at room temperature. Na_2FePO_4F crystallizes in the *Pbcn* space group and has two crystallographically unique sodium sites. All of the sodium from one of these sites is completely deintercalated upon charging of the material in an electrochemical cell. The unit cell of the oxidized compound ($NaFePO_4F$) is only 4% smaller than that of Na_2FePO_4F. The sodium can be extracted and reversibly replaced with lithium *in situ* in the cell. Furthermore, by an ion-exchange process, the entire Na content may be replaced with Li to yield Li_2FePO_4F, which has a slightly higher redox potential than the parent compound Na_2FePO_4F because of the more electropositive nature of the lithium compared to sodium. The small change in unit cell volume upon oxidation and reduction, room temperature solid solution behavior and multifunctional ion properties make Na_2FePO_4F a promising, and interesting material for Na- or Li-based cells.

The compound is *not* isostructural with known compounds Li_2CoPO_4F,[14] Li_2NiPO_4F,[15] or Na_2MnPO_4F,[16] which adopt very different layered (Co, Ni), and 3D (Mn) structures, respectively. However, the structures of some fluorophosphates that are analogous to Na_2FePO_4F have been reported previously, although the refinement statistics were very poor.[17,18] The comparable Co and Mg compounds also crystallize in the *Pbcn* space group and apparently have unusual structural features: the M^{2+} (M = Mg, Co) cations form face-sharing dimers and each sodium environment is claimed to be seven-coordinate. The structure of Na_2FePO_4F has not previously reported by single crystal methods, and is described here. The alkali ion-exchange characteristics were investigated in order to postulate a mechanism for ionic transport within these materials, and obtain a better understanding of the charge−discharge voltage characteristics vis a vis solid solution behavior. The latter also prompted our investigation of electron localization in this interesting system, which was studied by temperature dependent Mössbauer spectroscopy of the mixed valence single phase $Na_{1.5}FePO_4F$, and compared to the behavior of two phase $FePO_4$−$LiFePO_4$. Na_2FePO_4F was synthesized by new solid-state and hydrothermal routes to produce carbon-coated nanocrystallites that exhibit good rate behavior. Furthermore, other compounds of the type Na_2MPO_4F, including Na_2CoPO_4F, and Na_2NiPO_4F, were synthesized as single phase powders for the first time. We show that substitution of these M^{+2} cations, including Mg^{2+} into Na_2FePO_4F produces solid solutions of the type $Na_2(Fe_{1-y}M_y)PO_4F$, which exhibit distinct voltage plateau for the two transition metals at their respective redox potentials. The behavior of the nonisostructural Na_2MnPO_4F is also reported.

Experimental Section

Single Crystal Diffraction Analysis of Na_2FePO_4F. A 0.150 × 0.096 × 0.030 mm pale green crystal grown from placing FeO in a Na_2PO_3F flux was mounted on a nylon fiber with perfluoropolyether oil. Data were collected at 295 K using a Bruker APEX CCD platform diffractometer with monochromated Mo Kα (λ = 0.7107 Å) radiation. Data collection and reduction were performed with Bruker AXS SAINT and SMART5.0 programs, respectively. The final unit cell parameters were determined from 6924 reflections. A total of 1839 independent reflections were used for the structure solution and solved by least-squares structural refinement (F^2) using the Bruker SHELXTL package. Final R, wR(F^2), and GOF were 2.94%, 6.60%, and 1.417, respectively.

Synthesis of Polycrystalline Na_2MPO_4F: Solid State and Hydrothermal (M = Fe, Co, Ni, Mn). *Solid State*. Stoichiometric amounts of Na(CH_3COO), NaF and $NH_4H_2PO_4$ (or Na_2PO_3F for carbon-free methods) were ground in ceramic media in a planetary ball mill for 4−6 h with $Fe(C_2O_4)\cdot 2H_2O$, $CoCO_3$, $NiCO_3$, or $Mn(CH_3COO)_2\cdot 4H_2O$ to make compositions of $Na_2(Fe_x,Co_y,Ni_z)PO_4F$, ($x + y + z = 1$) or Na_2MnPO_4F. The samples were then treated at 350 °C for 4−6 h under flowing Ar to decompose the precursors. The powders were then subjected to further milling for 4−6 h, followed by a final heat treatment at 500−625 °C for 4−6 h.

Hydrothermal. Ten milliliters of a 0.30 M solution of H_3PO_4 was added to 10.0 mL of a 0.30 M solution of $(NH_4)_2Fe(SO_4)_2$, $CoCl_2$, or $MgCl_2$. The solution was basified with 0.9 g NaF and 1.2 g NaOH. The mixture was sealed in a 43 mL Teflon-lined

(9) United States Geological Survey *Mineral Commodity Summaries 2008*; Interior Dept. Geological Survey: Washington, DC, 2009.
(10) Stevens, D. A.; Dahn, J. R. *J. Electrochem. Soc.* **2001**, *148*, A803–A811.
(11) Barker, J.; Saidi, Y. M.; Swoyer, J. L. *J. Electrochem. Soc.* **2003**, *150*, A1394–A1398.
(12) Barker, J.; Saidi, M. Y.; Swoyer, J. L. *Electrochem. Solid-State Lett.* **2003**, *6*, A1–A4.
(13) Barker, J.; Gover, R. K. B.; Burns, P.; Bryan, A. J. *Electrochem. Solid-State Lett.* **2006**, *9*, A190–A192.
(14) Okada, S.; Ueno, M.; Uebou, Y.; Yamaki, J. *J. Power Sources* **2005**, *146*, 565–569.
(15) Dutreilh, M.; Chevalier, C.; El-Ghozzi, M.; Avignant, D.; Montel, J. M. *J. Solid State Chem.* **1999**, *142*, 1–5.
(16) Yakubovich, O. V.; Karimova, O. V.; Mel'nikov, O. K. *Acta Crystallogr. C* **1997**, *C53*(4), 395–397.
(17) Sanz, F.; Paradab, C; Ruiz-Valero, C. *J. Mater. Chem.* **2001**, *11*, 208–211.
(18) Swafford, S. H.; Holt, E. M. *Solid State Sci.* **2002**, *4*, 807–812.

Parr reactor and heated to 170−220 °C, where the product forms under autogenous pressure. The powders were then heated at 500−625 °C for 4−6 h under an Ar atmosphere. Sol−gel Na_2FePO_4F was prepared as previously outlined.[8]

Chemical Oxidation. Microcrystalline pure Na_2FePO_4F was oxidized with stoichiometric amounts of NO_2BF_4 in acetonitrile for 1 h to obtain the desired sodium content. Microcrystalline pure Na_2MnPO_4F was stirred with stoichiometric amounts of NO_2BF_4 in acetonitrile for 15 h.

Ion Exchange. Samples of Na_2FePO_4F were refluxed in acetonitrile with LiBr under a nitrogen atmosphere for 1−24 h. Samples of Na_2CoPO_4F were mixed with LiBr and placed in a 23 mL Teflon-lined Parr reactor, using ethanol as the solvent. The reactor was heated to 225 °C for 7 h.

Materials Characterization. Powder X-ray diffraction data of all materials was collected on a Bruker D8-Advantage powder diffractometer using Cu Kα radiation (λ = 1.5405 Å) operating from 2θ = 10° to 80°. Lattice parameters were determined by Treor 90 indexing software or GSAS,[19] using full pattern matching, followed by Rietveld refinement where indicated. SEM samples were gold coated and examined in a LEO 1530 field-emission scanning electron microscope (FESEM) instrument equipped with an energy dispersive X-ray spectroscopy (EDX) attachment. Images were recorded at 10 kV with a backscattered electron detector. EDX spectra were collected on regions of sample which measured 30 × 40 μm with an estimated sample penetration of 1 μm. The quantified data for each region is accurate to ±5%. The elemental composition of a sample was determined by averaging the data from at least five regions within a given sample. Inductively coupled plasma mass spectroscopy (ICP-MS), as per EPA 3050, was also used to determine Li/Na ratios.

Electrochemical Testing. Samples of electrochemically active materials were mixed with carbon black and polyvinylidene fluoride in a 75:15:10 weight ratio. The cell loading was 6 mg/cm^2. The electrochemical performance was evaluated using 2220 coin cells, using a lithium metal anode and 1 M $LiPF_6$ in a 1:1 ethylene carbonate/dimethyl carbonate electrolyte solution. Room temperature galvanostatic cycling was performed between 2.0 and 4.5 V for Na_2FePO_4F and $Na_2(Fe_{0.9}Mg_{0.1})PO_4F$; between 3.5 and 5.0 V for Na_2CoPO_4F and between 2.0 and 5.0 V $Na_2(Fe_{0.5}Co_{0.5})PO_4F$.

Thermal Gravimetric Analysis. Samples (10−20 mg) were placed in an alumina crucible and heated at 10 °C/min under N_2 (100 mL/minute) using an SDT Q-600 TGA from TA Instruments.

Mössbauer Spectroscopy. Mössbauer spectra were collected using a 50 mCi ^{57}CoRh source mounted on a constant-acceleration spectrometer calibrated using α-Fe foil at room temperature.[20] Fitting was accomplished using standard least-squares methods. For variable temperature experiments, spectra were measured in an increasing temperature sequence in increments of 50 °C with an equilibration time of 4 h followed by a counting time of 20 h ensuring that the spectra reflect the equilibrium state of these materials. A second series was run offset by the first by 25 °C to check for consistency and look for aging effects.

Results and Discussion

Refinement of Single Crystal Data. Na_2FePO_4F is a member of a class of A_2MPO_4F compounds that crystallize in the orthorhombic space group *Pbcn*. It is structurally similar to the hydroxy-phosphate $Na_2FePO_4(OH)$[21] and is isostructural with Na_2MgPO_4F[18] and Na_2CoPO_4F.[17] The previous reports of these two fluorophosphates compounds described important structural information but the refinements had uncommonly high residual error values. Therefore single crystals of Na_2FePO_4F were grown by a flux method to verify the details of this unusual framework.

Table 1. Lattice Constants and Atomic Parameters of Na_2FePO_4F from Single Crystal Data

Na_2FePO_4F				
Pbcn (Orthorhombic), Z = 8				
M_w = 215.80 g/mol				
D = 3.365 g cm^{-3}				
a = 5.2200(2) Å				
b = 13.8540(6) Å				
c = 11.7792(5) Å				
V = 851.85(6) Å^3				
atom	x	y	z	occ.
Fe	0.2275(1)	0.0101(1)	0.3261(1)	1.0
P	0.2035(1)	0.3810(1)	0.0871(1)	1.0
Na (1)	0.2633(1)	0.2446(1)	0.3281(1)	1.0
Na (2)	0.2395(1)	0.1249(1)	0.0836(1)	1.0
F (1)	0	0.1238(1)	0.25	0.5
F (2)	0.5	0.1009(1)	0.25	0.5
O (1)	0.2663(2)	0.3882(1)	−0.0396(1)	1.0
O (2)	0.2846(2)	0.2837(1)	0.1330(1)	1.0
O (3)	−0.0905(2)	0.3948(1)	0.1027(1)	1.0
O (4)	0.3398(2)	0.4636(1)	0.1515(1)	1.0

The single crystal refinement data for Na_2FePO_4F are summarized in Table 1 (see Supporting Information for details and bond lengths and angles). Two different views of the structure are depicted in Figure 1a. Each iron center is 6-coordinate, with four oxygen ligands and two fluorine ligands per metal ion. What makes this structure distinct is the connectivity of the 6-coordinate metal centers: Na_2FePO_4F consists of pairs of face-sharing Fe octahedra, each coordinated to four oxygen and two fluorine ions. These $Fe_2O_6F_3$ bioctahedral units are connected by corner-sharing (via F2) to other pairs of Fe face-shared octrahedra along the *a* direction, as shown in Figure 1a. These chains of Fe octahedra are connected through corner-sharing of PO_4^{3-} tetrahedra along the *c* direction. Bond lengths are given in Table 2. The phosphate tetrahedra are very regular with P−O bond distances ranging between 1.51 and 1.56 Å. There are two crystallographically unique sodium sites, Na1 and Na2, as indicated in Figure 1a. The Na1 site is surrounded by four oxygen ion (Na−O distances between 2.36 and 2.46 Å) and two fluorine ions. The Na−F bond lengths are 2.35 and 2.52 Å. Note there is an extra neighboring oxygen ion located 2.93 Å from Na1, which makes a small contribution to the valence bond sum of Na1. This [6 + 1] coordination of the Na1 ion is similar to that seen for sodium in $Na_2BeB_2O_5$.[22] Pairs of face-shared Na1 polyhedra corner-share via bridging fluorine ions (F1) in the *a* direction. The Na2 environment is slightly smaller than

(19) Toby, B. H. *J. Appl. Crystallogr* **2001**, *34*, 210–213.
(20) Data were collected exactly as in ref 2. The sample was equilibrated for 4 h prior to the 20 h data collection period. Each component was fitted with an independent line width to accommodate possible differences in disorder within each phase, and to allow for the dynamic broadening of the solid solution phase.
(21) Kabalov, Y, K.; Simonov, M. A.; Belov, N. V. *Dokl. Adak. Nauk SSSR* **1974**, *215*, 850–853.
(22) Li, W.; Ye, N. *Acta Crystallogr. E* **2007**, *E63*, i160.

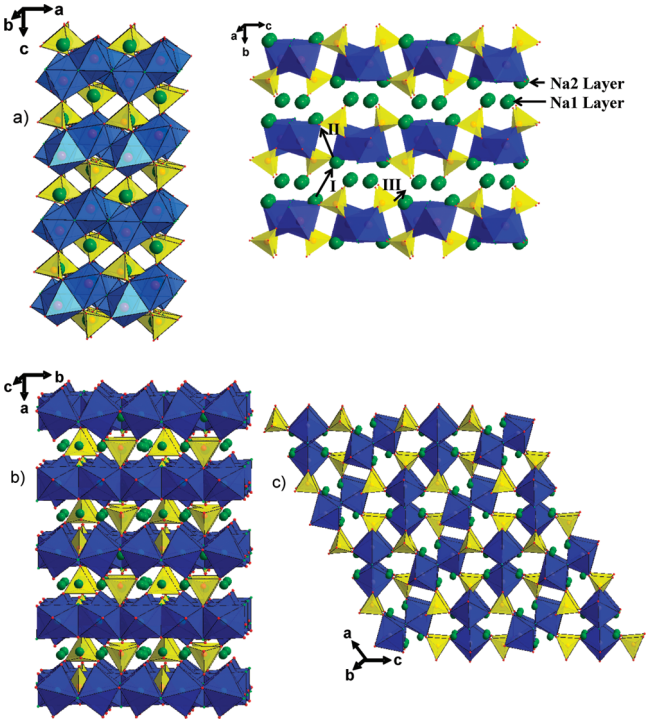

Figure 1. Crystal structure of Na_2FePO_4F (referred to in the text as structure **S1**): (a) view along [010] and along [100]. Ion transport pathways (I, II, and III) are marked. (b) The crystal structure of Li_2CoPO_4F (structure **S2**) and (c) the structure of Na_2MnPO_4F (structure **S3**). The transition metal octahedra are shown in blue, phosphate tetrahedra in yellow, and alkali ions in green.

that of Na1. The Na2 site has four oxygen ligands with Na−O bonds varying from 2.28 to 2.53 Å and two fluorine ligands, 2.32 and 2.41 Å from Na2. There is also an additional oxygen atom 2.80 Å from Na2. As a result, Na2 may be classified as having [6 + 1] coordination, much like Na1.

The refined single crystal unit cell parameters for Na_2FePO_4F (a = 5.2200(2) Å, b = 13.8540(6) Å, and c = 11.7792(5) Å) result in a unit cell volume of 851.85 Å^3. This is slightly larger than the unit cell of Na_2CoPO_4F (a = 5.2475(9) Å, b = 13.795(2) Å, c = 11.689(2) Å, V = 846.2 Å^3)[17] because of the larger ionic radius of Fe^{2+} (78 pm) compared to that of Co^{2+} (74 pm).[23] Although the cobalt coordination site is smaller than that of the iron site, the Na1 and Na2 environments are similar for both compounds.

It is noteworthy that the materials of the same "2111" stoichiometry, namely A_2MPO_4F (A = Li, Na; M = Co, Ni, Fe, Mn) crystallize in three different structures as a result of the subtle effects of ion size mediated interactions and magnetic interactions. The structures of the layered Na_2FePO_4F (structure **S1**, isostructural with the Co and Mg compounds), the "stacked" Li_2CoPO_4F[14] (structure **S2**), isostructural with Li_2NiPO_4F,[15] and the 3D Na_2MnPO_4F[16] (structure **S3**) are depicted in Figure 1a−c, respectively. Although location of the transition metal in octahedral sites is common to all three, the connectivity of the octahedra runs the entire gamut from mixed face-shared

(23) Shannon, R. D. *Acta Crystallogr. A* **1976**, *A32*, 751–767.

Table 2. Selected Atomic Distances in Na_2FePO_4F from Single Crystal Data

atoms	distance (Å)	atoms	distance (Å)
Fe1−O3	2.0382(11)	Na1−F1	2.3525 (11)
Fe1−F2	2.0997(8)	Na1−O2	2.3641(13)
Fe1−O1	2.1196(11)	Na1−O3	2.4109(13)
Fe1−O4	2.1404(11)	Na1−O1	2.4149(13)
Fe1−F1	2.1674(9)	Na1−O2	2.4643(13)
Fe1−O4	2.1832(11)	Na1−F2	2.5171(12)
		Na1−O2	2.9467(14)
Fe−Fe	2.9760(4)		
		Na2−O2	2.2882(13)
P1−O2	1.5128(11)	Na2−F1	2.3247(7)
P1−O1	1.5313(11)	Na2−O3	2.3828(13)
P1−O4	1.5463(11)	Na2−F2	2.4083(7)
P1−O3	1.5576(12)	Na2−O4	2.4088(13)
		Na2−O1	2.5307(14)
		Na2−O1	2.8039(14)

and corner-shared in **S1** to edge-shared in **S2** and corner-shared in **S3**. Considering the structures in which the alkali and TM is the same, namely, Na_2FePO_4F (**S1**) versus Na_2MnPO_4F (**S3**), the similar radii of Fe^{2+} (78 pm) compared to Mn^{2+} (83 pm) suggest that the two structures might be more closely related. However, although Fe^{2+}, Mg^{2+}, and Co^{2+} are clearly stable in a face sharing arrangement, the high spin state of Mn^{2+} (d^5), and the slightly larger size appears to result in unfavorable thermodynamics. Thus a different framework is adopted. In the case where the TM is the same, namely, Na_2CoPO_4F (**S1**) vs Li_2CoPO_4F (**S2**), the effects of the alkali prevail. The size of a Na^+ ion is 1.3 times than of a Li^+ ion, and thus we would not expect these two structures (prepared at high temperatures under thermodynamic control) to be the same. However, as was well established by *chimie douce* concepts long ago,[24] ion exchange of one alkali for another at low temperatures can produce metastable compounds with the **S1** structure such as Li_2FePO_4F and Li_2CoPO_4F, as long as the ion interactions are not highly destabilized within the resulting lattice. Full understanding of these considerations could be used to predict framework dimensionality and connectivity of polyanion-based lattices.

Synthesis of Na_2FePO_4F Polycrystalline Powders. Polycrystalline powders of Na_2FePO_4F can be produced by a sol−gel method as described previously.[8] Here we describe new one-pot hydrothermal methods and a solid-state route.

In the hydrothermal reaction, the reagents are sealed inside a Teflon-lined Parr reactor in alkaline aqueous media and heated to temperatures up to 220 °C under autogenous pressure, similar to the synthesis procedure for $LiFePO_4$.[25] The X-ray diffraction pattern is shown in Figure 2a. The lattice parameters are virtually identical to those of the single crystal. The Na/P/Fe/F ratio was confirmed to be 2:1:1:1 by elemental dispersive X-ray (EDX) analysis in the scanning electron microscope (SEM). The morphology of the product is shown in the SEM image in Figure 2b. The resultant particles are rod-like, typically 75−100 nm in the two thin dimensions and

(24) Figlarz, M. *Chem. Scr.* **1988**, *28*, 3–7.
(25) Yang, S.; Zavalij, P. Y.; Whittingham, M. S. *Electrochem. Commun.* **2001**, *3*, 505–508.

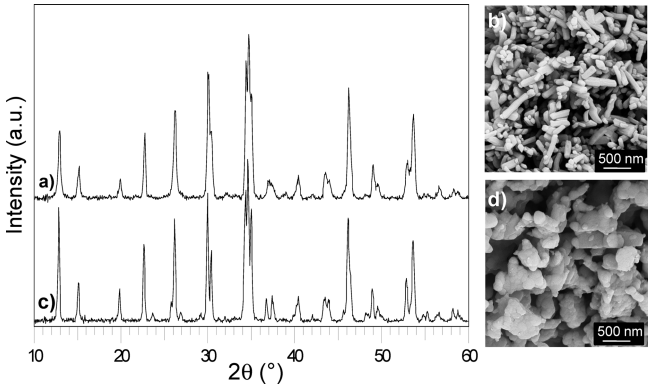

Figure 2. Powder diffraction patterns and corresponding SEM micrographs of Na_2FePO_4F (a) and (b) prepared hydrothermally (lattice parameters a = 5.231 Å, b = 13.887 Å, c = 11.806 Å); (c and d) prepared by a solid-state route (lattice parameters: a = 5.218 Å, b = 13.854 Å, c = 11.779 Å).

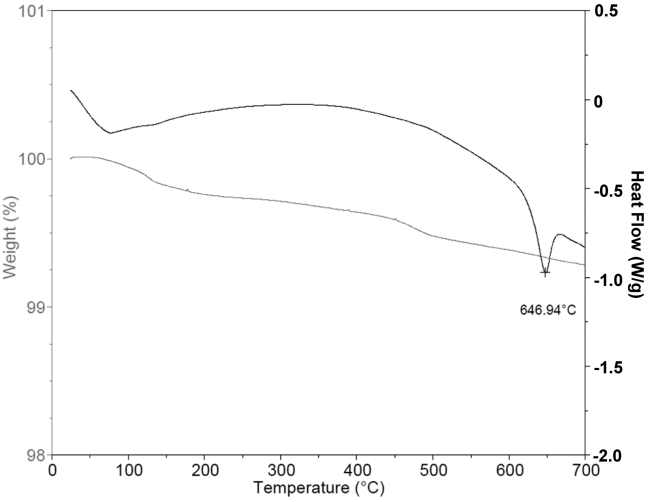

Figure 3. Thermal gravimetric analysis of carbon-containing solid state Na_2FePO_4F.

300−700 nm in the longest dimension. This anisotropic particle shape is not unexpected for a compound which has two long crystallographic axes (b and c) and one short axis (a). It is also a consequence of the specific nucleation and crystal growth conditions in the hydrothermal bomb, since the sol−gel and solid state routes (see below) provide much more isotropic crystallites. The solid-state route involves the mechanical grinding of solid precursors followed by heat treatment in a furnace under inert atmosphere. The resulting X-ray diffraction pattern is shown in Figure 2c. Again, the lattice parameters are very close to those of the single crystal. The morphology of Na_2FePO_4F prepared by the solid-state route using a carbon containing precursor (Fe oxalate) is shown in Figure 2d. The sample is comprised of large agglomerates (up to 800 nm) that are composed of smaller particles about 50−200 nm in size. Approximately 2% carbon is contained within the material based on TGA analysis (in air). Thermal gravimetric analysis of a solid-state sample was performed in an inert (nitrogen) atmosphere up to 700 °C, showing there is an endothermic event at 646 °C (Figure 3). Clearly, the compound decomposes in this temperature region under an inert atmosphere to produce NaF, Na_3PO_4, Fe and Fe_3O_4 (XRD data, not shown). In contrast, $LiFePO_4$ is more thermally robust. Carbothermal reduction occurs at a much higher temperature for $LiFePO_4$ (near 800 °C),[26] and hence formation of conductive sp^2 carbon and/or conductive phosphides is much more difficult for Na_2FePO_4F than for the olivine. We note that since Na_2FePO_4F decomposes near 650 °C, it would be virtually impossible to synthesize this compound directly at a temperature of 750 °C by a carbothermal route as described in a previous report,[27] although a carbothermal synthesis method is possible for $LiFePO_4$,[28] because of the greater thermal stability of the olivine.

Electrochemistry and Ion Exchange of Na_2FePO_4F with Lithium. Electrodes comprised of carbon-free (hydrothermal) Na_2FePO_4F were charged and discharged in a lithium cell with metallic Li as the negative electrode, at a rate of 1 Li in 10 h (C/10). The first electrochemical cycle is shown in Figure 4a. The discharge capacity of the first cycle is only 65 mAh/g, roughly half of the theoretical capacity. Similar results were obtained for the material prepared by the solid state route. Nonetheless, the capacity can be dramatically improved by coating the surface with carbon. In the case of $LiFePO_4$, this can also result in partial carbothermal reduction at elevated temperatures to form conductive iron phosphocarbides or phosphides such as metallic FeP. In tiny quantities (<1−3%), these, combined with carbon, may facilitate surface electron transport in $LiFePO_4$.[29] However, this is problematic for Na_2FePO_4F owing to the similar temperature of carburization, carbothermal reduction and compound decomposition as described above. We carbon coated hydrothermally prepared materials by adding organic reagents such as sucrose or ascorbic acid directly to the hydrothermal reactor that decompose and leave a carbonaceous coating on the surface. The material was then heat-treated between 550 and 700 °C to carburize the surface coating without inducing carbothermal decomposition. The resultant Na_2FePO_4F contained about 2 wt % carbon. The first cycle of a cell is shown in Figure 4a, and initial results of a cell cycled at a C/10 rate at room temperature are shown in the inset of Figure 4b. The material exhibits a sloping potential in a Li-ion electrolyte with an average potential of 3.3 V (versus Li metal). The voltage is slightly higher than that calculated for this material in a Na-ion cell, but similar to that for Li_2FePO_4F.[30] The reversible capacity of 115 mAh/g is about 85% of the theoretical capacity, and it displays the same stability as the sol−gel derived Na_2FePO_4F (reported previously, for 50 cycles). It shows better rate capability (cells charged at C/10 and discharged at faster

(26) Ellis, B.; Herle, P. S.; Rho, Y.-H.; Nazar, L. F.; Dunlap, R.; Perry, L. K.; Ryan, D. H. *Faraday Discuss.* **2007**, *134*, 119–141.
(27) Barker, J.; Saidi, M. Y.; Swoyer, J. L. US Patent 6,872,492, **2005**.
(28) Barker, J.; Saidi, M. Y.; Swoyer, J. L. *Electrochem. Solid-State Lett.* **2003**, *6*, A53–A55.
(29) Rho, Y.-H.; Nazar, L. F.; Perry, L.; Ryan, D. *J. Electrochem. Soc.* **2007**, *154*, A283–A289.
(30) Ramzan, M.; Lebegue, S.; Ahuja, R. *Appl. Phys. Lett.* **2009**, *94*, 151904−1–151904−3.

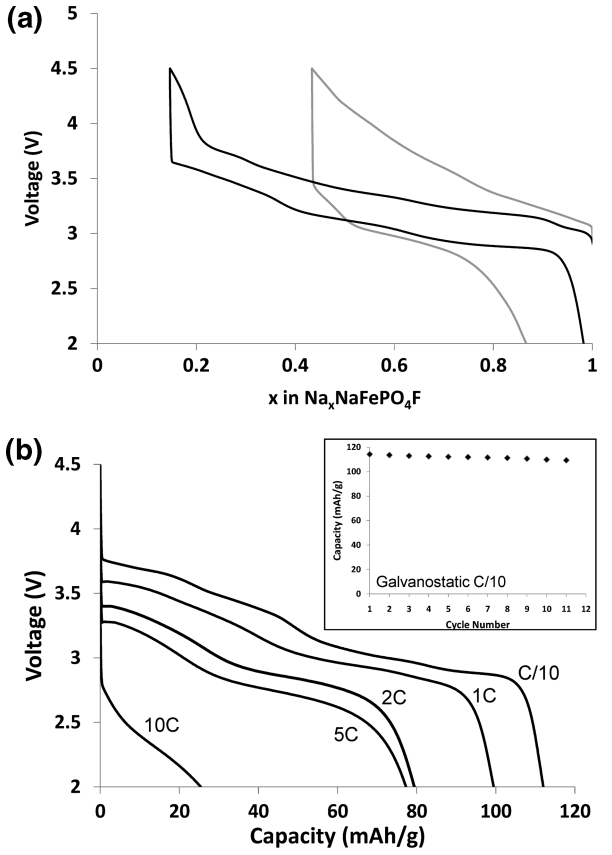

Figure 4. (a) Electrochemical curve of Na_2FePO_4F (cycled in a lithium cell *vs* metallic Li at a rate of *C*/10) prepared by a carbon-free hydrothermal technique (gray curve) and by a hydrothermal route containing 2% carbon (black curve). (b) Rate performance of carbon-containing hydrothermally prepared Na_2FePO_4F at various discharge rates after charging at a rate of *C*/10. Inset: Capacity retention data for cycling at *C*/10.

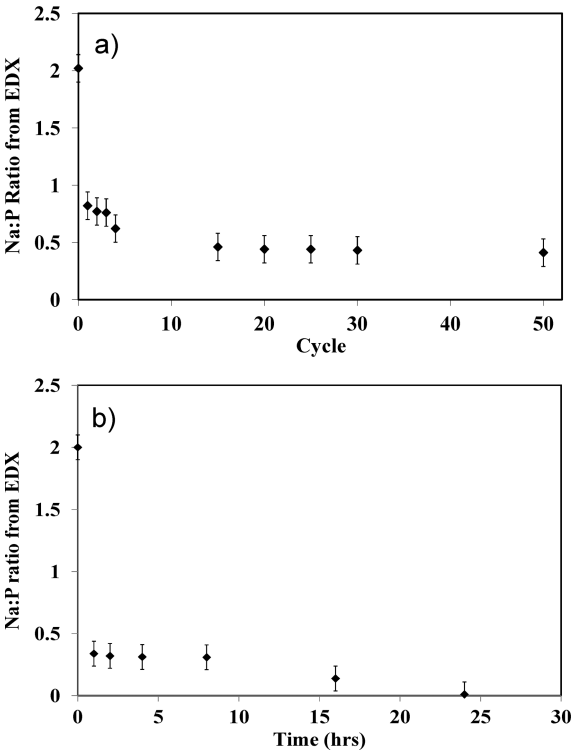

Figure 5. Na:P ratios determined by EDX analysis of crystallites in the FESEM. (a) Na_2FePO_4F material taken from electrochemical cells cycled *vs* Li metal as a function of cycle number. (b) Na_2FePO_4F after ion exchange with LiBr in acetonitrile as a function of exchange time.

rates, Figure 4b), that is, a capacity of about 80 mAh/g at 5C (discharge in 12 min) was achieved. This is indicative of the benefits a thin carbon coating provides this material. We anticipate substantial improvements in electrochemical properties for smaller particles and improved coatings, which is work in progress.

Electrochemical cycling of Na_2FePO_4F versus a Li negative electrode using $LiPF_6$ electrolyte has been shown to be a method of Na/Li ion exchange.[8] Elemental analysis of the positive electrode material scraped from multiple cells after cycling at a slow rate (C/10) was performed using EDX, the results of which are shown in Figure 5a. Analysis conducted on the positive electrode after the first discharge (Li insertion) revealed that the Na:P ratio is close to 1:1, indicating a chemical formula of (Li,Na)$FePO_4F$. This indicates that 1 mol of Na was extracted on the initial charge, followed by the insertion of 1 mol of Li during the initial discharge. Since Na1 sites are isolated from each other, any deviation from a 1:1 Na:P ratio would imply exchange between the Na1 and Na2 sites. Indeed, this is the case on longer cycling. In a cell halted after five cycles, the Na/Li ratio continued to decline and $Li_{1.4}Na_{0.6}FePO_4F$ was formed. Although ion exchange between the Na1 and Na2 site occurs, not all of the sodium in the Na1 site exchanges during the course of slow electrochemical cycling. The electrode in a cell after 50 cycles still contained 20% of the original sodium content.

Moreover, ion exchange was also observed when a cell based on Na_2FePO_4F versus Li was equilibrated at open circuit voltage (OCV) in $LiPF_6$-EC/DMC. At the outset, the cell had an open circuit potential of 2.960 V, but this dropped slowly to 2.905 V after 72 h. The potential remained constant at 2.905 V for another 48 h, at which point the cell was dismantled. The material was scraped from the positive electrode and thoroughly washed. Analysis showed the Na/P ratio was 1:1; thus half of the Na was exchanged for lithium even without cycling the cell.

More forcing conditions of ion exchange, such as solvent reflux with a lithium salt, are necessary to fully convert Na_2FePO_4F into the metastable Li_2FePO_4F phase. Ion exchange of Na_2FePO_4F with Li was performed by refluxing Na_2FePO_4F with LiBr in acetonitrile. Using EDX analysis, the sodium content with respect to reflux time was measured (Figure 5b). The exchange proceeds very quickly in the initial stages and after only 1 h, only 30% of the initial sodium remains. After 24 h of reflux, the sodium signal is no longer present in the EDX spectrum indicating that the exchange has gone to completion.

A closer look at the sodium layers of the Na_2FePO_4F structure reveals important details about ion exchange vis a vis sodium (or lithium) ion mobility. As the oxidized compound $NaFePO_4F$ contains sodium only in the Na1 site,[8] it suggests that Na2 is the more mobile ion. Inspection of the two virtually identical frameworks reveals at least three potential paths for ion transport

Table 3. Lattice Parameters for Sol−Gel $Na_{2-x}FePO_4F$ Prepared by Chemical Oxidation of Na_2FePO_4F

compound	space Group	*a* (Å)	*b* (Å)	*c* (Å)	*β* (deg)	*V* (Å^3)
Na_2FePO_4F	*Pbcn*	5.2372(5)	13.8587(7)	11.779(1)	90	854.93
$Na_{1.75}FePO_4F$	*Pbcn*	5.219	13.893	11.602	90	841.23
$Na_{1.5}FePO_4F$	*P*2/*c*	13.929(6)	5.200(9)	11.514(7)	91.22(2)	834.03
$Na_{1.25}FePO_4F$	*Pbcn*	5.204	13.910	11.478	90	830.87
$NaFePO_4F$	*Pbcn*	5.1018(7)	14.1224(6)	11.360(1)	90	818.48

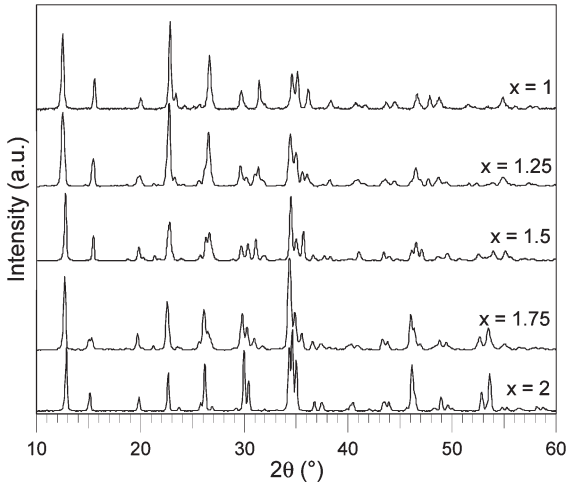

Figure 6. X-ray diffraction patterns of Na_xFePO_4F illustrating the solid-solution behavior of the system in the range from $x = 2 \rightarrow 1$ prepared by chemical oxidation using $NOBF_4$.

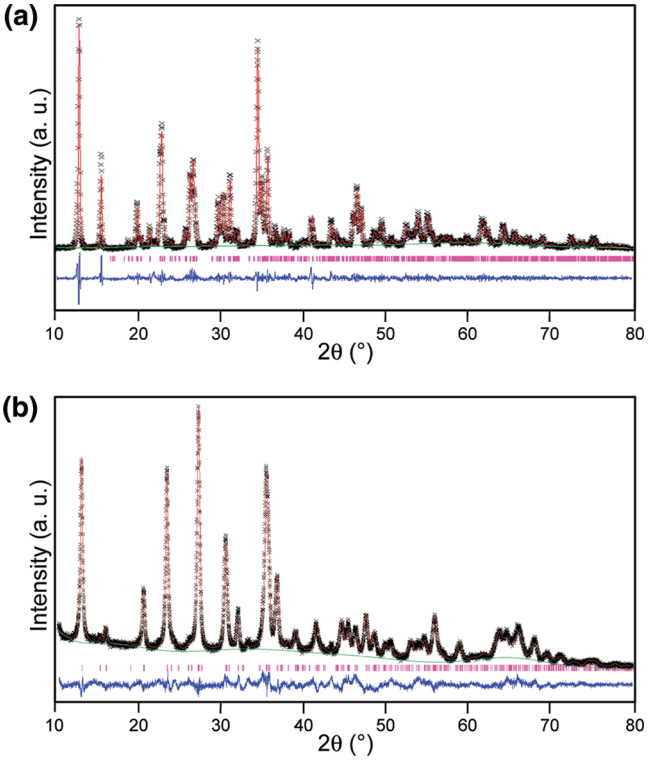

Figure 7. (a) LeBail XRD refinement of $Na_{1.5}FePO_4F$ in *P*2/*c*, wRp = 9.07%: lattice parameters $a = 13.929(6)$ Å, $b = 5.200(9)$ Å, $c = 11.514(7)$ Å; $\beta = 91.22°$. (b) Rietveld refinement of $Li_{1.25}Na_{0.75}FePO_4F$, synthesized from $NaFePO_4F$ reduced with excess LiI in *Pbcn*, wRp = 7.69%: lattice parameters $a = 5.0327(3)$ Å, $b = 13.8590(7)$ Å, $c = 11.2081(5)$ Å. For each, the fit is shown in red, the calculated reflections are shown in magenta, the background fit is shown in green and the difference map is shown in blue.

(see Figure 1a). Pathway I involves displacement primarily in the *b*-direction with small displacements in the *a* and *c* directions. The two Na2 sites are 4.7 Å apart and are separated by a large irregularly shaped interstitial site. Pathway II is similar to pathway I in that the primary displacement is also in the *b* direction with small displacements in the *a* and *c* directions. The distance between the two Na2 sites along Pathway II is approximately 4.7 Å, and the two sites are separated by an irregular interstitial site. Pathway III is simply displacement along the *a* axis by one unit cell length (5.22 Å). Pathway III is not a straight pathway however: an iron atom and an oxygen atom (O1) partially obstruct transport (see Figure 1a). As a result, ion migration along this pathway may be less probable relative to pathways I and II. The shortest Na2−Na2 distance in the structure is 4.65 Å, but this pathway is obstructed by the two face-sharing Fe atoms. Each Na2 polyhedron shares a face with three Na1 polyhedra, each of which is between 3.25 and 3.32 Å from Na2. This allows exchange of alkali ions between Na1 and Na2. In the case of ion exchange with LiBr in refluxed acetonitrile, the exchange is sufficiently facile to replace all of the Na in the structure with Li.

Chemical Redox Studies of Na_2FePO_4F using Li and Na Reducing Agents. As we previously reported, Na_2FePO_4F may be chemically oxidized using NO_2BF_4 in a 1:1 ration, according to the reaction: $Na_2FePO_4F + xNO_2BF_4 \rightarrow Na_{2-x}FePO_4F + xNaBF_4 + xNO_2$.[8] The resulting diffraction patterns are shown in Figure 6, and lattice parameters are summarized in Table 3. The broadened features of some intermediate compositions prevented successful Rietveld refinement of their structures. $Na_{2-x}FePO_4F$ compounds appear to be have a wide range of nonstoichiometry and share similar structural features and lattice parameters with the parent compound. In the initial steps of oxidation ($Na_{2-x}FePO_4F$, $x < 0.25$), the orthorhombic *Pbcn* structure is maintained; the *a* and *c* lattice parameters contract while the *b* lattice parameter increases. Further oxidation results in $Na_{1.5}FePO_4F$, which is a single phase with lattice parameters intermediate between the two end members. The diffraction pattern and full pattern refinement is shown in Figure 7a. Extraction of half of the alkali results in a very small distortion in symmetry from the end member orthorhombic *Pbcn* cells, adopted by both Na_2FePO_4F and $NaFePO_4F$, to a *P*2/*c* monoclinic unit cell with lattice parameters intermediate between the two end-members. Because of the increase of β from 90° to 91.22°, Vegard's law is not precisely obeyed. The distortion in this single phase composition probably results from ordering of the Fe^{2+} and Fe^{3+} ions in the lattice (and/or the Na^+ ions), as has been observed in other mixed oxidation state

Table 4. Rietveld Refinement Results and Atomic Positions for $Li_{1.25}Na_{0.75}FePO_4F$ Synthesized from $NaFePO_4F$ Reduced with Excess LiI

$Li_{1.25}Na_{0.75}FePO_4F$					
wavelength (Å)				1.5405, 1.5443	
space group (No.)				*Pbcn* (60)	
a (Å)				5.0407(3)	
b (Å)				13.8069(9)	
c (Å)				11.2215(5)	
V (Å^3)				780.98(5)	
Z				8	
fitted Rwp (%)				7.48	
fitted Rp (%)				5.81	
χ^2				32.13	
R_f (%)				2.70	
atom	*x*/*a*	*y*/*b*	*z*/*c*	U_{iso}	occ.
Fe1	0.2521(9)	0.0048(4)	0.3307(3)	0.0053(6)	1.0
P1	0.231(1)	0.3723(6)	0.0780(6)	0.0061(8)	1.0
Na1	0.288(3)	0.237(1)	0.3355(8)	0.0125	0.591(5)
Li1	0.288(3)	0.237(1)	0.3355(8)	0.015	0.409(5)
Na2	0.195(4)	0.137(2)	0.085(2)	0.0125	0.195(6)
Li2	0.195(4)	0.137(2)	0.085(2)	0.015	0.805(6)
F1	0	0.103(1)	0.25	0.026(2)	0.5
F2	0.5	0.129(2)	0.25	0.028(2)	0.5
O1	0.354(2)	0.384(1)	−0.042(1)	0.026(3)	1.0
O2	0.224(3)	0.2847(8)	0.1179(8)	0.023(2)	1.0
O3	−0.055(2)	0.393(1)	0.074(1)	0.015(3)	1.0
O4	0.370(3)	0.430(1)	0.162(1)	0.014(4)	1.0

phosphates such as $Li_2V^{+3}V^{+4}(PO_4)_3$.[31] This would likely occur via the formation of mixed oxidation state dimer pairs within the "2111" structure (see Figure 1). Detailed diffraction studies are underway for $Na_{2-x}FePO_4F$ and will be reported elsewhere.

Further oxidation results in the structure reverting back to the orthorhombic *Pbcn* space group. The lattice parameters of $NaFePO_4F$ show that the unit cell volume of 818.48 Å^3 is only 4% smaller than that of the parent compound Na_2FePO_4F. Overall, there is a clear trend in the lattice parameters: the *a* and *c* lattice parameters contract while the *b* lattice parameter increases. Transition between these two closely related phases results in "solid-solution-like" electrochemical behavior over the redox range that is spanned by $Na_{2-x}FePO_4F$ ($x = 0 \rightarrow 1$), and the phase transition from the orthorhombic phase to the monoclinic phase at $x = 0.5$ is not readily observable in the electrochemical profile of the hydrothermal material in Figure 4a. Likely, the electrochemical profile is complicated by the Li/Na ion exchange that takes place in the cell at room temperature (see above).

As described earlier, oxidation of Na_2FePO_4F to form $NaFePO_4F$ results in removal of all of the sodium from the Na2 site, while the Na1 site remains fully occupied. $NaFePO_4F$ may be reduced chemically using alkali metal iodides since the potential of $NaFePO_4F$ is greater than 2.7 V. Reduction with NaI reproduces the parent compound Na_2FePO_4F as expected, but reduction with *excess* LiI results in a composition $Li_{1.25}Na_{0.75}FePO_4F$, as shown by the 0.6:1 Na:Li ratio obtained from elemental analysis using ICP. A Rietveld refinement of the X-ray diffraction pattern of this sample is shown in Figure 7b. The atomic positions of sodium and lithium were constrained to be identical while the total occupancy of each alkali cation site was constrained to one. The isotropic thermal parameters for Li and Na were fixed using typical literature values. A summary of the refinement results is shown in Table 4. The stoichiometry attained from the refinement was $Li_{1.22}Na_{0.78}FePO_4F$, in excellent accord with the chemical analysis. The lattice parameters were refined to be $a = 5.0407(3)$ Å, $b = 13.8069(9)$ Å, $c = 11.2215(5)$. As expected, the unit cell volume of this compound (780.98 Å^3) is significantly less than that of Na_2FePO_4F (854.93 Å^3), and the sodium occupancy shows that ion scrambling has occurred: approximately 0.2 Na are situated on the Na2 site and only 0.6 Na remain on the Na1 site. Clearly, there is transport of sodium in the lattice from the Na1 site to the previously unoccupied Na2 site. We conclude that not only has LiI reduced $NaFePO_4F$ to $LiNaFePO_4F$, but some of the remaining Na has ion exchanged with the excess LiI. This is in accordance with the room-temperature ion-exchange observed for a cell at OCV (see above). We believe that disordered Na/Li occupation contributes to the sloping voltage profile.

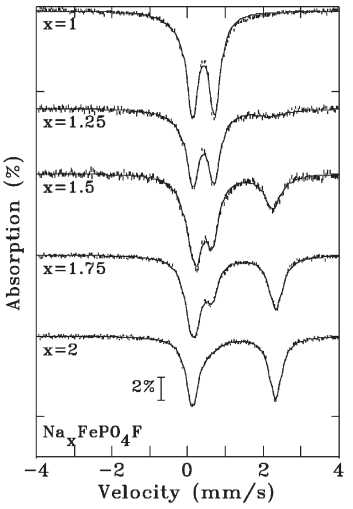

Figure 8. Room-temperature Mössbauer data of Na_2FePO_4F, $Na_{1.75}FePO_4F$, $Na_{1.5}FePO_4F$, $Na_{1.25}FePO_4F$, and $NaFePO_4F$ prepared by chemical oxidation of Na_2FePO_4F.

Mössbauer Studies of $Na_{1.5}FePO_4F$. Room temperature Mössbauer measurements (Figure 8) on materials prepared by a sol−gel route confirm the oxidation state of the iron. In Na_2FePO_4F, there is one dominant signal with an isomer shift (IS) of 1.16 mm/s and a quadrupole splitting (QS) of 2.20 mm/s, typical of Fe^{2+} in an octahedral environment. Approximately 4 mol % of Fe^{3+} was also detected in the sample, possibly the result of surface oxidation, or a small amount of an amorphous Fe^{3+} impurity. Chemical oxidation results in a decrease in the Fe^{2+} signal intensity that exactly correlates with the increase in the Fe^{3+} signal as expected, up to the formation of $NaFe^{3+}PO_4F$ (IS = 0.43 mm/s, QS = 0.48 mm/s). Further oxidation is made difficult by the inaccessibly high redox couple anticipated for the $Fe^{3+/4+}$ couple.

Temperature-dependent Mössbauer studies were performed on the target compound $Na_{1.5}FePO_4F$ to investigate whether thermally activated small polaron hopping occurs

(31) Yin, S. C.; Grondey, H.; Strobel, P.; Nazar, L. F. *J. Am. Chem. Soc.* **2003**, *125*, 326.

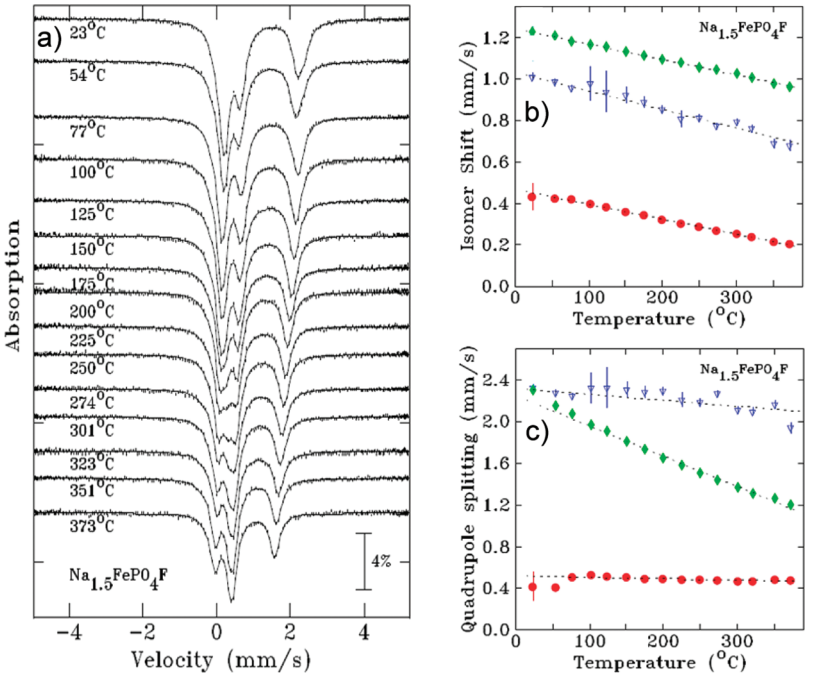

Figure 9. (a) Fitted variable-temperature Mössbauer data of $Na_{1.5}FePO_4F$ from room temperature to 373 °C with a summary of (b) isomer shifts and (c) quadrupole splittings at various temperatures. The Mossbauer data for the majority Fe^{2+} component are plotted as green diamonds, "defect" Fe^{2+} component as blue triangles, and the Fe^{3+} component as red circles.

in this mixed Fe^{2+}/Fe^{3+} single phase on the Mössbauer time scale (about 10^{-8} s). Analysis of the room-temperature data shows the expected 50:50 ratio of the Fe^{3+}/Fe^{2+} components (Figure 9a) for $Na_{1.5}Fe^{2+/3+}PO_4F$. The Fe^{3+} component (IS = 0.43 mm/s, QS = 0.4 mm/s) is identical to that of $NaFePO_4F$ as expected. The Fe^{2+} signal was split into two components: the majority (45%) exhibits typical Fe^{2+} parameters (IS = 1.23 mm/s, QS = 2.31 mm/s). The remaining Fe^{2+} signal (5%; IS = 1.01 mm/s and QS = 2.32 mm/s) we ascribe to surface or defect Fe^{2+} sites that lack full octahedral coordination. The fitted Mössbauer spectra recorded on increasing the temperature up to 373 °C are shown in Figure 9a. For each point, a 4 h thermalization time was employed, followed by a counting time of 20 h, giving an overall time of one day per temperature point. Thus, each experiment in the temperature range between room temperature and 373 °C was recorded over the period of two interleaved 7-day runs. The spectrum of each sample is dominated by the contributions of the parent Fe^{2+} and Fe^{3+} phases. The Mössbauer parameters derived from the fitting the $Na_{1.5}FePO_4F$ spectra at the different temperatures are summarized in Figures 9b−c. The standard thermal dependence of the isomer shifts of each of the three components is observed over the entire range of temperatures probed. Furthermore, the relative area of each signal did not change as the sample was heated. These are the only components that exist over this temperature range: no new spectral features that would correspond to rapid electron hopping on the Mössbauer time scale emerged at any temperature. Upon cooling the sample back to room temperature the original spectrum was fully recovered.

In contrast, a transition to a solid solution regime for bulk $Li_{0.5}FePO_4$ occurs above 200 °C.[2] We have previously described temperature-dependent Mössbauer studies for the olivine system described by the two phase system, $LiFePO_4/FePO_4$ where the onset of rapid small polaron hopping on the Mössbauer time scale was correlated exactly with the onset of Li disordering among the lattice sites to form a single phase solid solution $Li_{0.5}FePO_4$.[2] At room temperature, Li^+ ion and electron hopping are a coupled activated process that occurs across the grain boundary between the two phases ($LiFePO_4$ and $FePO_4$; which adopt the same space group). At 220 °C, entropy drives the collapse of the phase boundary, and both lithium and electrons disorder within the solid solution lattice. However, $Na_{1.5}FePO_4F$ is a single phase that exhibits a structural distortion to a monoclinic space group *vis a vis* its orthorhombic end-members (Na_2FePO_4F and $NaFePO_4F$). This is undoubtedly the result of electron localization in the system to form Fe^{2+}/Fe^{3+} sites (see above). Additional energy would be required to remove the distortion and hence average the two sites to $Fe^{2.5+}$. We note that the effects of the structural distortion and iron valence ordering do not preclude electron hopping between neighboring Fe^{2+}/Fe^{3+} sites which may occur at a slower rate ($< 10^{-8}$ s) than the Mössbauer time scale can measure.

Synthesis of Na_2CoPO_4F Polycrystalline Powders. In manner similar to that of Na_2FePO_4F, polycrystalline samples of Na_2CoPO_4F can also be prepared by solid-state or hydrothermal routes. According to the Ellingham diagrams detailing carbothermal reduction,[32] Co^{2+} may be reduced to metallic Co at temperatures near 300 °C, which is well below that of our solid-state firing temperature. We have observed that Na_2CoPO_4F is very susceptible to carbothermal reduction. All attempts to use

(32) Evans, J. W.; DeJonghe, L. C. *The Production of Inorganic Materials*; Macmillan: New York, 1991.

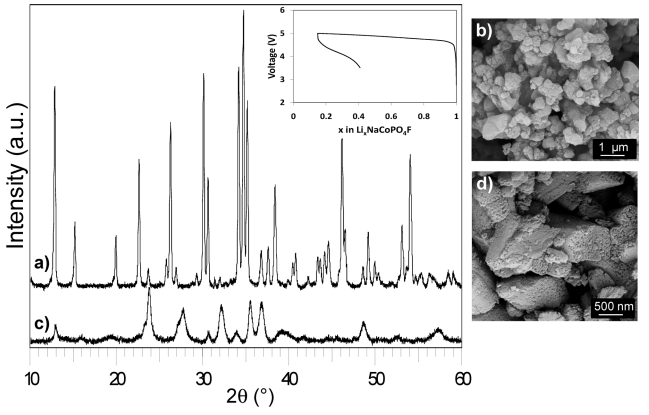

Figure 10. Powder diffraction patterns and corresponding SEM micrographs of Na_2CoPO_4F (a) and (b) prepared by a carbon-free solid-state route (c) and (d) ion-exchanged for 7 h. Inset: First electrochemical profile of Na_2CoPO_4F cycled at a rate of $C/10$.

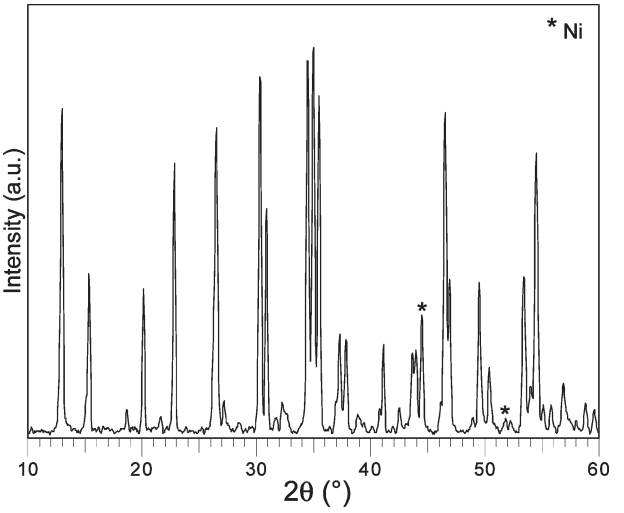

Figure 11. X-ray powder diffraction pattern of Na_2NiPO_4F, with Ni impurity peaks noted.

carbon-containing precursors for the synthesis, such as cobalt acetate, produced elemental cobalt that was clearly evident in the diffraction pattern. Therefore a carbon-free solid-state method was employed. The diffraction pattern is shown in Figure 10a and the corresponding lattice parameters are in Figure 11. Comparison of refined powder X-ray data for Na_2CoPO_4F and Na_2FePO_4F shows that the two Na sites (Na1 and Na2) in both compounds are almost identical. The unit cell volume of 843.1 Å^3 differs from the original report by Sanz[17] by 0.3% and EDX measurements confirms a Na/Co/P/F ratio of 2:1:1:1. The product consists of particle agglomerates which range up to 750 nm in diameter, as seen in the SEM micrograph in Figure 10b. A solvent-reflux method of ion exchange of Na_2CoPO_4F was not sufficiently forcing to produce a complete exchange of Na for Li in the material. Thus a pressurized ion exchange was performed using a solution of LiBr and ethanol, which yielded Li_2CoPO_4F. The resultant diffraction pattern is shown in Figure 10c. The broad diffraction peaks and weak signal-to-noise ratio clearly indicate the crystallinity of the material has decreased. This is confirmed by an SEM image of the particle surface (Figure 10d). Distinct cracking of the particles is observed. The difficulty in ion-exchange indicates a reduced ability for sodium ion transport through the lattice. However, Na_2CoPO_4F has a unit cell volume almost 2% less than that of Na_2FePO_4F: this increased crystallographic density may inhibit facile motion of ions.

Comparison of the diffraction patterns from Na_2CoPO_4F and Li_2CoPO_4F produced from ion-exchanged Na_2CoPO_4F clearly show that the ion-exchanged material maintains the structural features of the **S1** structure (Figure 1a). But not surprisingly, this form of Li_2CoPO_4F is metastable. Heating it compound to 580 °C under an Ar flow causes the structure to revert back to the thermodynamically stable form of Li_2CoPO_4F: the **S2** layered structure.

Electrochemistry of Na_2CoPO_4F. Electrochemical cycling of Na_2CoPO_4F (using Li as a counter electrode) was performed at a very slow rate (C/10), with the voltage profile of the first cycle shown in Figure 10 (inset). It exhibits a long sloping first charge profile between 4.7 and 5.0 V, at which point 85% of the capacity was reached, although some of this capacity is probably the result of electrolyte oxidation. The discharge capacity was very low compared to that of the overall capacity as only 25% of the material was discharged. The poor reversible capacity of sodium cobalt fluorophosphate is similar to that reported for $LiCoPO_4$.[33]

Substitution: Other Phases of Na_2MPO_4F (M = Fe, Co, Ni, Mg, Mn). Although Mg, Co and Fe variants of Na_2MPO_4F are known, Na_2NiPO_4F is not. We synthesized this material by the solid-state route and its diffraction pattern is shown in Figure 11. This compound is also sensitive to reduction, since trace amounts of elemental Ni were found in the diffraction pattern even with the usage of carbon-free precursors. Na_2NiPO_4F is clearly isostructural with the aforementioned Mg, Co, and Fe sodium fluorophosphates. Na_2NiPO_4F has a unit cell volume of 823.4 Å^3 which is 4% smaller than that for Na_2FePO_4F and 1.5% smaller than that for Na_2CoPO_4F, owing to the smaller size of the nickel ion compared to the other transition metal ions. An electrochemical cell which contained Na_2NiPO_4F as the positive electrode material did not show any electrochemical activity below 5 V. It is expected that this compound has a Ni^{2+}/Ni^{3+} redox couple above 5 V, similar to that of other nickel phosphates such as $LiNiPO_4$[34] and Li_2NiPO_4F.[14]

Although electrochemical inactivity may be anticipated for Na_2NiPO_4F up to 5 V, surprising was the complete lack of electrochemical activity we observed for carbon-containing Na_2MnPO_4F. Although this material is not isostructural with Na_2FePO_4F, the structure (**S3**, Figure 1c) suggests that open pathways should be available for Na mobility, most notably in the *b*-direction where Na ions are situated along tunnels within the structure. The material was prepared by a solid-state method similar to that for

(33) Amine, K.; Yasuda, H.; Yamachi, M. *Electrochem. Solid-State Lett.* **2000**, *3*, 178–179.
(34) Wolfenstine, J.; Allen, J. *J. Power Sources* **2005**, *142*, 389–390.

Na_2FePO_4F which involved vigorous ball-milling of the precursors for up to 12 h and produced agglomerates of small particles. The final Na_2MnPO_4F product contained roughly 3% carbon by mass, owing to the use of manganese acetate as a precursor. Despite these efforts, the material did not exhibit any electrochemical activity below 5 V. Furthermore, the solid state prepared Na_2MnPO_4F was also found to resist chemical oxidation: no reaction was observed upon stirring the material with NO_2BF_4 for 15 h. Studies into the further reduction of the particle size of Na_2MnPO_4F to overcome possible limitations of ion-transport of this material are ongoing.

Substitutional solid solution compounds of the type $Na_2(Mg_w,Fe_x,Co_y,Ni_z)PO_4F$, $(w + x + y + z = 1)$ can also be directly synthesized hydrothermally or by a solid-state route. Single phase compounds of the solid solution $Na_2(Fe_{1-x}Co_x)PO_4F$ are observed by X-ray diffraction and the lattice parameters are summarized in Figure 12. The individual lattice parameters follow a clear trend upon substitution of Co for Fe: the *a* lattice parameter increases, while those for *b* and *c* decrease. However, these trends are not linear and do not strictly follow Vegard's law. Similar compounds are also known for lithium phospho-olivines: substitutional solid solutions of M2 site ions have been synthesized as lithium-ion battery materials by various solid-state and hydrothermal routes, and remain of particular interest for electrochemical study.[35−37] Initial electrochemical results for $Na_2(Fe_{1-x}Co_x)PO_4F$ compounds cycled up to 5 V versus Li show two distinct regions of redox potential (near 3.3 and 4.7 V) but minimal reversibility is demonstrated. Preliminary results for $Na_2(Fe_{1-x}Mg_x)PO_4F$ ($x < 0.15$) compounds show electrochemical profiles similar to those for Na_2FePO_4F, with only slight performance improvement upon doping with Mg. In the case of $Li(Fe_{1-x}Mg_x)PO_4$, Mg doping up to 15% has been shown to substantially improve the performance of the olivine.[38] This may be in part a result of the lesser unit cell volume difference between the end members, which reduces lattice strain. For example, $Li(Fe_{0.90}Mg_{0.1})PO_4$ and $Li_{0.1}(Fe_{0.90}Mg_{0.10})PO_4$ exhibit a volume difference of only 5.15%, close to that reported for high-rate $LiFePO_4$ nanocrystallites and much less than for the bulk material, of 6.5%.

Conclusions

Na_2FePO_4F is a new electrode material in a family of known sodium metal fluorophosphates that crystallize in the space group *Pbcn*. The single crystal data confirms the unique structural features of the structure, including the [6 + 1] pseudo-octahedral geometry of both Na sites in the lattice and the face-sharing dimers of iron atoms. Both Na_2FePO_4F and isostructural Na_2CoPO_4F can be synthesized a variety of methods, including sol−gel, hydrothermal, and high-temperature solid-state routes. Carbon-coated hydrothermally synthesized Na_2FePO_4F exhibits particularly promising electrochemical properties. Furthermore, electrochemically active, high cell voltage, substitutional solid solutions of the form $Na_2(Mg_w,Fe_x,Co_y,Ni_z)PO_4F$, $(w + x + y + z = 1)$ may be prepared. However, compositionally identical, but structurally distinct Na_2MnPO_4F exhibits very poor electrochemical behavior despite an open pathway for alkali migration. Further studies are underway to understand this phenomenon more fully.

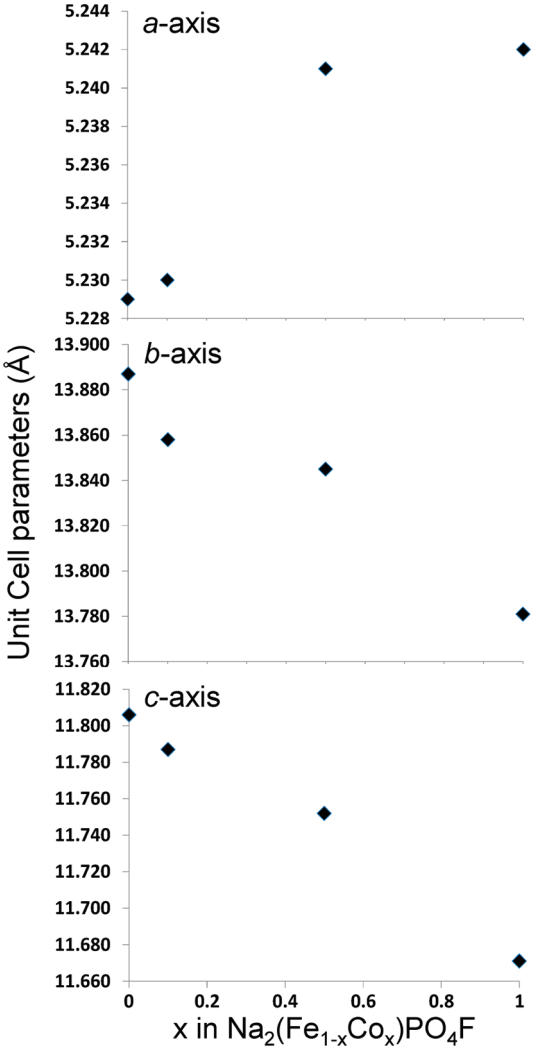

Figure 12. Lattice parameters for single-phase solid-solution compounds $Na_2(Fe_{1-x}Co_x)PO_4F$.

Na_2FePO_4F can be reversibly cycled in an electrochemical cell with lithium as the counter electrode at rates up to 5*C*. Ion exchange of Na_2FePO_4F and this series of compounds is accomplished by several methods including by reflux with a Li salt, and in a Li cell by electrochemical exchange, or by simple equilibration at OCV. The propensity of these sodium fluorophosphates to undergo ion exchange demonstrates the high mobility of the alkali ions in the lattice. In sharp contrast to the olivine $LiFePO_4$, distinct two phase behavior on cycling is not observed. The $Na_{1.5}FePO_4F$ phase intermediate between the two orthorhombic end-members Na_2FePO_4F and

(35) Yamada, A.; Kudo, Y.; Liu, K.-Y. *J. Electrochem. Soc.* **2001**, *148*, A1153–A1158.
(36) Chen, G.; Wilcox, J. D.; Richardson, T. J. *Electrochem. Solid-State Lett.* **2008**, *11*, A190–A194.
(37) Ellis, B.; Kan, W. H.; Makahnouk, W. R. M; Nazar, L. F. *J. Mater. Chem.* **2007**, *17*, 3248–3254.
(38) Wang, D.; Li, H.; Shi, S.; Huang, X.; Chen, L. *Electrochim. Acta* **2005**, *50*, 2955–2958.

$NaFePO_4F$, exhibits a slight monoclinic distortion, with lattice parameters that are intermediate between those of the two end-members. The distortion appears to be driven by electron localization of Fe^{2+}/Fe^{3+} in $Na_{1.5}FePO_4F$ (at least at time scales on the order of 10^{-8} s) as confirmed by temperature-dependent Mössbauer measurements. Na^+ ion ordering may also play a role. Intriguingly, in situ Na^+/Li^+ ion exchange in the electrochemical cell results in scrambling of the Na/Li ions and a sloping voltage profile suggestive of quasi-solid solution behavior. The complex interplay of ion-ordering/disordering and electron-localization/delocalization in this system will be the subject of our future investigations.

Acknowledgment. L.F.N. and D.R. acknowledge NSERC for financial assistance through the Discovery Grant Program. L.F.N. is grateful to General Motors and NSERC for funding through the Collaborative Research Program and to NSERC for generous support via a Canada Research Chair.

Supporting Information Available: Single-crystal data for Na_2FePO_4F. This material is available free of charge via the Internet at http://pubs.acs.org.